

Communication

NMR q -space imaging of macroscopic pores using singlet spin states

Nirbhay N. Yadav, Allan M. Torres, William S. Price*

Nanoscale Organisation and Dynamics Group, College of Health and Science, University of Western Sydney, Campbelltown Campus, Locked Bag 1797, Penrith South DC, NSW 1797, Australia

ARTICLE INFO

Article history:

Received 5 February 2010

Revised 1 March 2010

Available online 19 March 2010

Keywords:

Diffusion

 q -Space imaging

Singlet state

Restricted diffusion

ABSTRACT

NMR q -space imaging is a powerful non-invasive technique used to determine structural characteristics of pores in applications ranging from medical to material science. To date, the application of q -space imaging has primarily been limited to microscopic pores in part because of limitations of the effective observation time due to relaxation. Here we report on the use of singlet spin states for NMR q -space imaging, which allow significantly greater observation times. This opens the way for studying larger pores in materials such as biological tissue, emulsions, and rocks.

© 2010 Elsevier Inc. All rights reserved.

1. Introduction

In the standard NMR q -space method (pulsed gradient spin-echo; PGSE) [1–3], the position of molecules is encoded by magnetic field gradients at two instants in time separated by a delay Δ . The mean squared displacement (MSD) during Δ leads to an attenuation of the NMR spin-echo signal (E). For molecules diffusing in an infinite medium, the signal attenuation is a function of the effective area of the gradient pulses (q), diffusion coefficient (D), and Δ . When the molecules are within a confining geometry, the MSD is limited at long Δ by the size (and shape) of the pore hence the signal attenuation becomes sensitive to the pore dimensions. When $D\Delta/a^2 \sim 1$, where $2a$ is the characteristic distance of the pore, diffraction-like coherence features can be observed on a plot of E vs. q , i.e., ‘ q -space imaging’ [4]. Additionally, Fourier inversion of $E(q)$ yields further information on the restricting geometry. These coherence features only begin to appear when $D\Delta/a^2 \sim 1$ therefore the size of the pore effectively determines the required Δ duration or necessitates the use of molecules with much higher diffusion coefficients (i.e., hyperpolarised gases [5–6]). Nevertheless, to date q -space imaging using liquid molecules has only been applied to microscopic geometries (relatively small a values) due to limits on the duration of Δ .

The diffusion time (Δ) is normally limited by the time for the spins to lose phase coherence, either by spin–spin or spin–lattice relaxation in Hahn echo-based or stimulated echo-based PGSE sequences, respectively. The use of singlet spin states [7] to preserve nuclear spin order has recently been used to study the diffusion of

slow moving molecules [8] thus enabling an order of magnitude increase in the range of Δ . Here a singlet spin states pulse sequence (Fig. 1) is used to study the structural characteristics of cylindrical and rectangular pores. The results are compared with experiments using the pulsed gradient stimulated echo (PGSTE) pulse sequence [9].

2. Results and discussion

The signal attenuation from 50% 2,3-dibromothiophene in CDCl_3 diffusing between the planes of an NMR microtube (Fig. 2a, BMS-3; Shigemi, Tokyo) with interplanar spacing ($2a$) = 250 μm (measured using an optical microscope) and different Δ periods is shown in Fig. 2. The data in Fig. 2b is from experiments conducted using a PGSTE pulse sequence whilst Fig. 2c is from experiments using a singlet spin states pulse sequence. The relationship between larger Δ and more distinct coherence features is seen in both Fig. 2b and c however there is a difference in the location of the coherence features between the PGSTE and singlet spin states data. The location of the coherence features using a PGSTE sequence correspond to $2a$ = 250 μm (matching optical microscopy measurements) whilst the coherence features from the singlet spin states sequence correspond to $2a$ = 200 μm . The difference in echo attenuation between the PGSTE and singlet state data, which is not observed for separate peaks corresponding to 2,3-dibromothiophene diffusing freely along the sides of the tube, is thought to be due to different relaxation mechanisms once the molecules strike the surface of the planes [10]. Certainly wall relaxation effects are known to cause complications in the analysis of q -space measurements [10–12], and this hypothesis is supported by the diffusion coefficients (D_{app}) measured using PGSTE

* Corresponding author. Fax: +61 2 4620 3025.

E-mail address: w.price@uws.edu.au (W.S. Price).

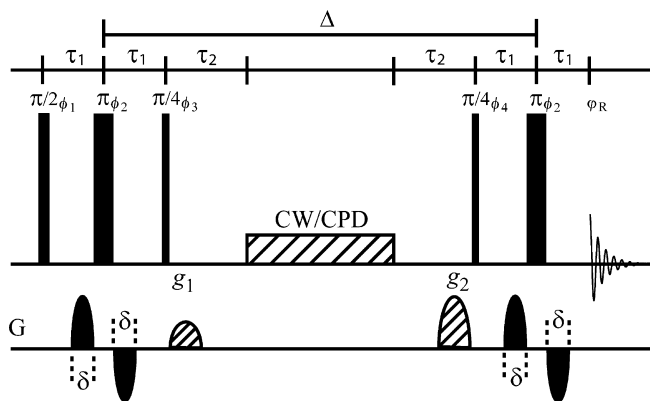


Fig. 1. Pulse sequence for Singlet-State pulsed gradient spin-echo (Singlet-PGSE). For a sample containing a scalar-coupled two-spin system (IS) with spin-coupling constant J_{IS} and chemical shifts ω_I and ω_S , the delays are $\tau_1 = 1/(4J_{IS})$ and $\tau_2 = \pi/|\omega_I - \omega_S|$. Rectangles with diagonal bars are implemented either as unmodulated RF field (continuous wave, CW) or as composite RF pulse decoupling (CPD). Pulsed gradient field g_1 and g_2 are used to remove unwanted coherences. $\phi_1 = x$, $\phi_2 = x$, $\phi_3 = x, y, -x, -y, -x, y, \phi_4 = x, y, -x, -y$, and $\phi_R = x, x, x, x, -x, -x, -x, -x$.

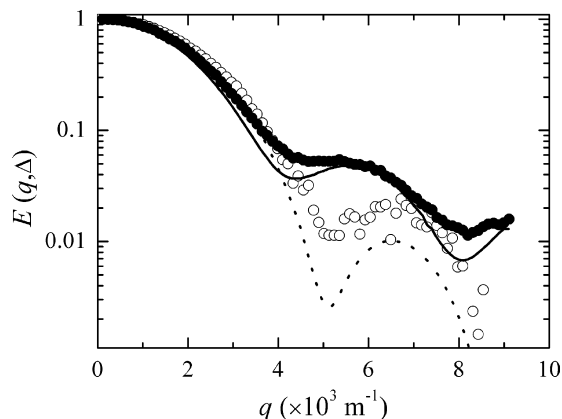


Fig. 3. Comparison between the PGSTE (●) and singlet spin state (○) experimental data for $\Delta = 15$ s. The coherences features in the singlet spin states data are shifted to higher q values as a consequence of additional surface relaxation. Eq. (1) was fitted by eye to the PGSTE and singlet spin state experimental data by setting $2a = 250 \mu\text{m}$, $\Delta = 15$ s, $D = 9 \times 10^{-10} \text{m}^2 \text{s}^{-1}$ and adjusting the wall relaxivity parameter M . M was set to zero when fitting to the PGSTE data (—) and $M = 3 \times 10^{-5} \text{m s}^{-1}$ gave the best fit for the singlet spin state data (- - -).

and singlet spin state pulse sequences diverging at larger Δ (i.e., as more molecules strike the surface).

A direct comparison between the PGSTE and singlet spin states data ($\Delta = 15$ s) along with simulated data for diffusion between planes is shown in Fig. 3. The echo signal attenuation incorporating spin relaxation at the surface for diffusion between planes is given by [11]

$$E(q, \Delta) = \sum_{n=0}^{\infty} \exp\left[-\frac{\xi_n^2 D \Delta}{a^2}\right] 2(1 + \sin(2\xi_n)/2\xi_n)^{-1} \times \frac{[(2\pi qa) \sin(2\pi qa) \cos \xi_n - \xi_n \cos(2\pi qa) \sin \xi_n]^2}{[(2\pi qa)^2 - \xi_n^2]^2} + \sum_{m=0}^{\infty} \exp\left[-\frac{\zeta_m^2 D \Delta}{a^2}\right] 2(1 + \sin(2\zeta_m)/2\zeta_m)^{-1} \times \frac{[(2\pi qa) \cos(2\pi qa) \sin \zeta_m - \zeta_m \sin(2\pi qa) \cos \zeta_m]^2}{[(2\pi qa)^2 - \zeta_m^2]^2} \quad (1)$$

where $2a$ is the interplanar spacing and the eigenvalues ξ_n and ζ_m are determined from the equations $\xi_n \tan(\xi_n) = Ma/D$ and $\zeta_m \cot(\zeta_m) = -Ma/D$, where M is the wall relaxivity parameter. As shown in Fig. 3, there is very good agreement between the experimental data and the fitted models indicating the observed coherence features are real. The difference between the intensity of the coherence minima is due to a polydispersity of the characteristic distances [13].

In an attempt to apply singlet spin states to larger pores, we measured the signal attenuation of 2,3-dibromothiophene diffusing within a stack of cylindrical capillaries (Fig. 4a) of diameter ($2a$) = 0.8 mm and $\Delta = 70$ s. The signal attenuation (Fig. 4b) exhibits multiexponential decay indicating restricted diffusion effects. The average propagator [14] $P(R, \Delta)$ obtained from Fourier inversion of the experimental data in Fig. 4b corresponds to an average pore diameter of ~ 0.8 mm.

We have shown that singlet spin states allow detection of restricted diffusion effects and q -space coherence features at very long Δ values thus greatly expanding the range of applicability of NMR q -space measurements. However, as only half of the total

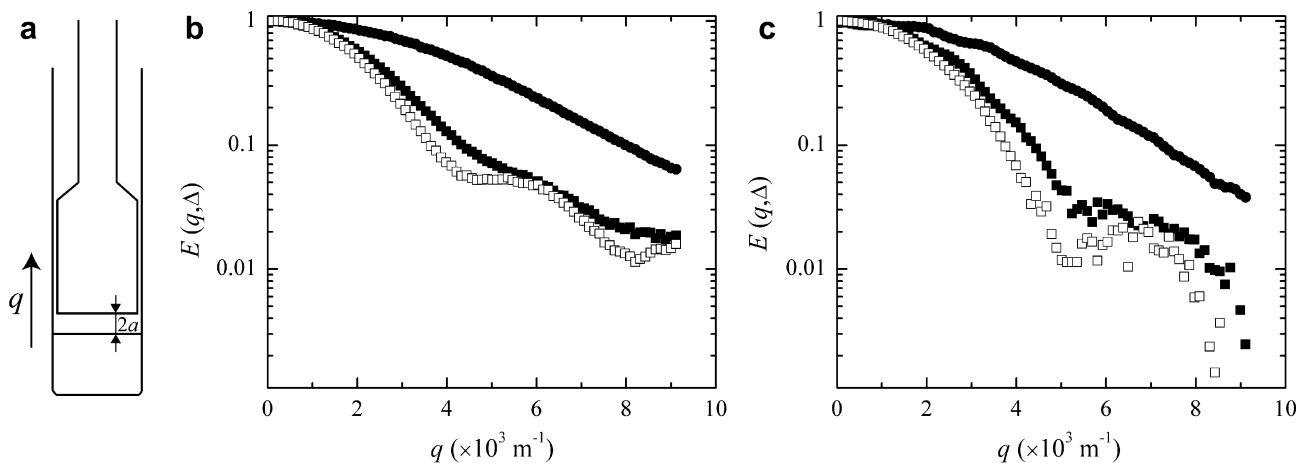


Fig. 2. (a) Schematic diagram of the rectangular pore created using a Shigemi NMR microtube. The gradient (q) is orientated perpendicular to the planes whilst $2a$ is the spacing between the planes. This arrangement produces molecules in two populations: (i) molecules diffusion between the bottom of the plunger and the bottom of the barrel and (ii) molecules diffusing freely along the sides and above the plunger. The sample volume between the planes is $\sim 3 \mu\text{L}$. (b) Signal attenuation from 2,3-dibromothiophene diffusing within an NMR microtube using PGSTE. (c) Singlet spin state pulse sequences for $\Delta = 2$ s (●), $\Delta = 10$ s (▲), and $\Delta = 15$ s (□). The diffraction minima in (a) correspond to $2a = 250 \mu\text{m}$ whilst (b) corresponds to $2a = 200 \mu\text{m}$.

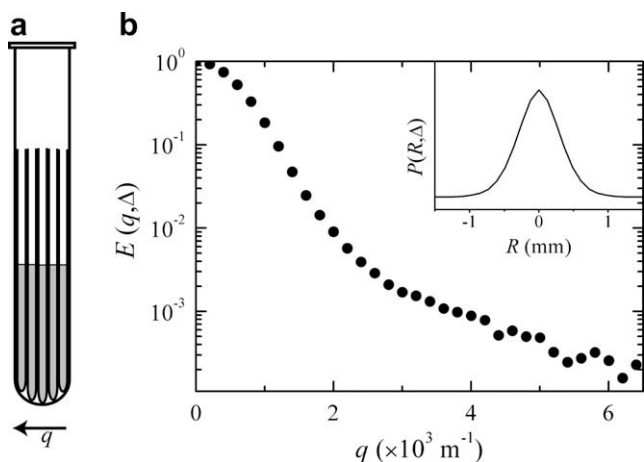


Fig. 4. (a) Schematic diagram of a stack of capillaries with diameter ($2a$) = 0.8 mm within an NMR tube. (b) Signal attenuation from 2,3-dibromothiophene diffusing within the capillary with $\Delta = 70$ s and gradients applied in the radial direction. The inset in (b) shows the average propagator $P(R, \Delta)$ obtained by Fourier inversion of the experimental data using Origin Pro 8 (OriginLab, Northampton). $P(R, \Delta)$ obtained from the experimental data matches the characteristic distance of the capillaries.

magnetisation is converted into singlet spin states in the pulse sequence [8] a PGSTE sequence will provide better sensitivity for relatively short Δ (see Figs. 2 and 3). The singlet-PGSE sequence is superior to PGSTE at Δ values beyond the limits imposed on PGSTE sequences by longitudinal relaxation (where $T_1 \sim 6$ s for this system). Indeed, diffusion measurements at time scales like those used in this study are impossible using PGSTE sequences.

Acknowledgments

This research was supported by a University of Western Sydney Postgraduate Award (N.N.Y) and a NSW BioFirst Award from the

NSW Ministry for Science & Medical Research (W.S.P.). We thank Dr. Tim Stait-Gardner and Dr. Gang Zheng for useful discussions.

References

- [1] E.O. Stejskal, J.E. Tanner, Spin diffusion measurements: spin echoes in the presence of a time-dependent field gradient, *J. Chem. Phys.* 42 (1965) 288–292.
- [2] P.T. Callaghan, A. Coy, D. MacGowan, K.J. Packer, F.O. Zelaya, Diffraction-like effects in NMR diffusion studies of fluids in porous solids, *Nature* 351 (1991) 467–469.
- [3] W.S. Price, *NMR Studies of Translational Motion*, Cambridge University Press, New York, 2009.
- [4] P.T. Callaghan, *Principles of Nuclear Magnetic Resonance Microscopy*, Oxford University Press, Oxford, 1993.
- [5] R.W. Mair, D.G. Cory, S. Peled, C.H. Tseng, S. Patz, R.L. Walsworth, Pulsed-field-gradient measurements of time-dependent gas diffusion, *J. Magn. Reson.* 135 (1998) 478–486.
- [6] R.W. Mair, G.P. Wong, D. Hoffmann, M.D. Hürlimann, S. Patz, L.M. Schwartz, R.L. Walsworth, Probing porous media with gas diffusion NMR, *Phys. Rev. Lett.* 83 (1999) 3324–3327.
- [7] M. Carravetta, O.G. Johannessen, M.H. Levitt, Beyond the T_1 limit: singlet nuclear spin states in low magnetic fields, *Phys. Rev. Lett.* 92 (2004) 153003.
- [8] S. Cavadini, J. Dittmer, S. Antonijevic, G. Bodenhausen, Slow diffusion by singlet state NMR spectroscopy, *J. Am. Chem. Soc.* 127 (2005) 15744–15748.
- [9] J.E. Tanner, Use of the stimulated echo in nmr diffusion studies, *J. Chem. Phys.* 52 (1970) 2523–2526.
- [10] A. Coy, P.T. Callaghan, Pulsed gradient spin echo nuclear magnetic resonance for molecules diffusing between partially reflecting rectangular barriers, *J. Chem. Phys.* 101 (1994) 4599–4609.
- [11] P.T. Callaghan, Pulsed-gradient spin-echo NMR for planar, cylindrical, and spherical pores under conditions of wall relaxation, *J. Magn. Reson. A* 113 (1995) 53–59.
- [12] W.S. Price, A.V. Barzykin, K. Hayamizu, M. Tachiya, A Model for diffusive transport through a spherical interface probed by pulsed-field gradient NMR, *Biophys. J.* 74 (1998) 2259–2271.
- [13] N.N. Yadav, W.S. Price, Effects of polydispersity on PGSE NMR coherence features, in: S. Brandani, C. Chmelik, J. Kärger, R. Volpe (Eds.), *Diffusion Fundamentals II*, Leipzig University Press, Berlin, 2007, pp. 40–51.
- [14] J. Kärger, W. Heink, The propagator representation of molecular transport in microporous crystallites, *J. Magn. Reson.* 51 (1983) 1–7.